



Article

# Reliability–Resiliency–Vulnerability Approach for Drought Analysis in South Korea Using 28 GCMs

Jang Hyun Sung <sup>1</sup>, Eun-Sung Chung <sup>2,\*</sup>  and Shamsuddin Shahid <sup>3</sup> 

<sup>1</sup> Han River Flood Control Office, Ministry of Environment, Seoul 06501, Korea; jhsung1@korea.kr

<sup>2</sup> Faculty of Civil Engineering, Department of Civil Engineering, Seoul National University of Science and Technology, Seoul 01811, Korea

<sup>3</sup> Faculty of Civil Engineering, Universiti Teknologi Malaysia (UTM), Johor Bahru 81310, Malaysia; sshahid@utm.my

\* Correspondence: eschung@seoultech.ac.kr; Tel.: +82-2-970-9017

Received: 24 July 2018; Accepted: 21 August 2018; Published: 27 August 2018



**Abstract:** This study developed a Reliability–Resiliency–Vulnerability (R–R–V) approach that aggregates the frequency, duration, and severity of droughts estimated using the Standardized Precipitation Evapotranspiration Index (SPEI). This approach was used to analyze the characteristics of droughts for the current (1976–2005) and the future (2010–2099) climates. The future climate data obtained from 28 general circulation models (GCMs) of Coupled Model Intercomparison Project Phase 5 (CMIP5) was divided into three general periods: Future 1: 2010–2039, Future 2: 2040–2069; and Future 3: 2070–2099. As a result, aggregation R–R–V representing water availability would increase during Future 1, and then gradually decrease until the end of the century. The frequencies of future drought events for Future 2 and Future 3 were similar to the current frequency, while the durations will be longer and the severity will be higher at most locations during Future 3. Thus, the mean of R–R–V over South Korea is expected to decrease, except for Future 1, and the spatial variability of R–R–V is expected to increase. In the end, the changes in the mean and variance of rainfall and temperature would lead to a decrease in the mean and increase in the spatial variation of sustainability in South Korea. This approach and its results can be used to establish a long-term drought strategy for regions where the risk of future drought is expected to increase.

**Keywords:** Coupled Model Intercomparison Project Phase 5 (CMIP5), drought analysis; Reliability–Resiliency–Vulnerability (R–R–V) approach; Standardized Precipitation Evapotranspiration Index (SPEI)

## 1. Introduction

Extreme events due to climate change have been frequent worldwide. According to survey results by the Pew Research Center, among the climate change-induced natural hazards, concern about drought was the largest regardless of the continents, followed by flood and heat waves [1]. Globally, the necessities of the adaptation strategies for climate change have been required due to concerns about the decrease in sustainability in water resources. Therefore, an assessment of sustainability in water resources for future drought scenarios is very important.

The consideration of uncertainties of climate change in impact analysis, vulnerability assessment, and adaptation strategies is generally regarded as a necessity in climate change study, because any single climate model cannot reliably represent the future climate condition. Thus, various methods have been developed to select proper general circulation models (GCMs) based on their performances to simulate the current climates. However, the best regeneration performance of the current climate does not correspondingly guarantee the precision of GCMs to simulate future climates. In recent

years, an ensemble approach has been proposed to include the future simulation of a large number of GCMs [2,3]. This use of multiple GCMs can be a good way to reduce the uncertainty inherent in climate change projection by a number of GCMs [4–6].

The simulated climates of GCMs are usually downscaled at the station level or high-resolution grid points using a dynamic or statistical approach for impact assessment at the local or regional scale. The dynamic downscaling can consider the interaction between climatic systems and non-stationarity due to the climate change, because the locality of climate forcing is generally included in the regional climate models (RCMs). In addition, the spatio-temporal correlation between variables can be interpreted based on the physics of the Earth system. On the other hand, statistical downscaling focuses on the statistical relationships between simulated climate values and historical observations, which may not be valid in the future [7–9]. On the other hand, statistical downscaling is much flexible, easy, and less time-consuming compared to dynamic downscaling [10]. To overcome the limitations of statistical downscaling and the complexity of dynamic downscaling, hybrid downscaling procedures have been developed and applied in recent years [11–13]. Especially, NASA Earth Exchange Global Daily Downscaled Projections (NEX-GDDP) and Downscaled CMIP3 and CMIP5 climate and Hydrology Projections (DCHP) provided an improved statistical downscaling based on Bias-Correction/Spatial Disaggregation (BCSD), which maintained the long-term trends inherent in GCMs [11]. Thus, this method has been widely used for the projection of future climates [12,14,15].

The main characteristics of drought events are duration and severity, which can be numerically defined by any drought index. Recent studies have widely used the bivariate copular method to consider these two variables at the same time [16,17]. However, since the occurrence frequency is generally accepted as another important variable, it should be considered in the analysis of drought. From this perspective, Zongxue et al. [18] proposed a hazard index that takes into account frequency, severity, and duration at the same time, and Loucks et al. [19] suggested an aggregation approach including three variables.

In this study, a Reliability–Resiliency–Vulnerability (R-R-V) approach for drought analysis is used through the aggregation index using the Standardized Precipitation Evapotranspiration Index (SPEI). This index was used to assess the possible changes in drought characteristics of Korea due to the plausible climate changes from 28 GCMs. This approach can be used to analyze the future drought characteristics in order to establish the long-term drought strategies for any region.

## 2. Data and Methodology

### 2.1. Procedure

The simulated climates from various GCMs were used to project the changes in SPEI over South Korea (Figure 1). The climate simulations of 28 GCMs provided by Coupled Model Intercomparison Project Phase 5 (CMIP5) were downscaled for 60 meteorological stations of Automatic Synoptic Observation System (ASOS) for this purpose. This downscaling method was based on the long-term trend of climate simulations (Figure 2). In order to project the change of drought characteristics, reliability, resiliency, and vulnerability were calculated for four periods: one current period (~1976–2005), and three future periods (~2010–2039, Future 1; ~2040–2069, Future 2; and ~2070–2099, Future 3). This study employed Representative Concentration Pathway (RCP) 4.5 for the projection of climate. RCP4.5 is a medium-concentration scenario that implies the stabilization of radiative forcing at 4.5 Watts/m<sup>2</sup> in the year 2100. The application of the RCP4.5 can provide a common platform for climate models to explore the climate system response to stabilizing the anthropogenic components of radiative forcing [20]. RCP4.5 is a mitigation scenario that was assumed a general scenario for South Korea considering the response to climate change through regulation [21].

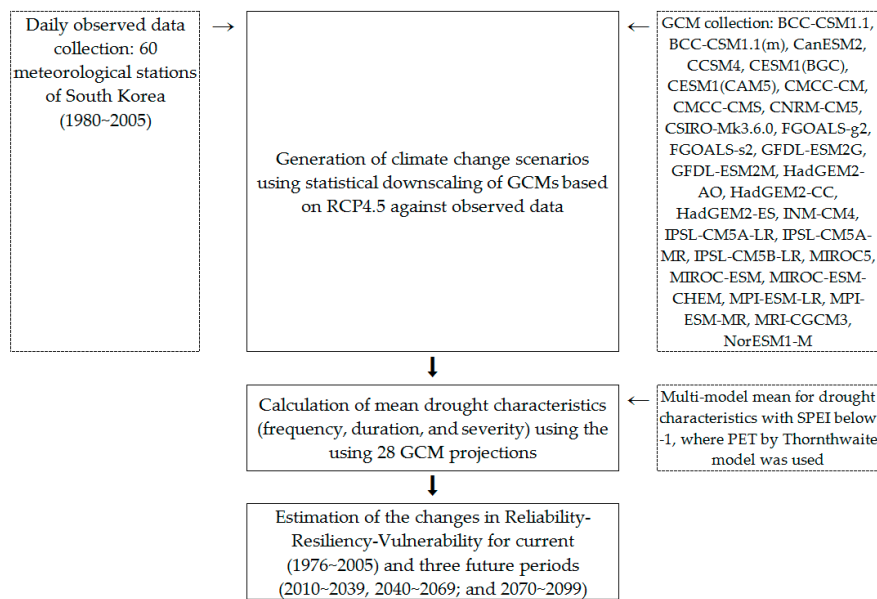


Figure 1. Procedure used to assess sustainability under future drought scenarios.

### 2.2. Statistical Downscaling of GCM Simulations

APCC (APEC Climate Center) Integrated Modeling (AIMS) produced downscaled climate projection data of South Korea using two BCSD methods [22]. These are the SQM (Simple Quantile Method) and Spatial Disaggregation with Quantile Delta Mapping [SDQDM, 15] which can preserve the long-term temporal trends in climate. This study used the downscaled future projections of daily precipitation and temperature of 28 GCMs of the Coupled Model Intercomparison Project Phase 5 (CMIP5) for RCP4.5 at 60 ASOS meteorological stations of South Korea (Figure 1) provided by AIMS. Table 1 lists the 28 GCMs used in this study.

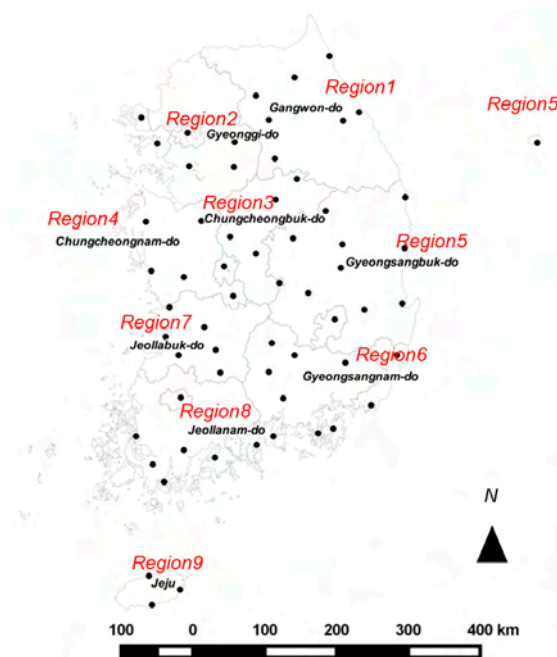


Figure 2. Locations of 60 Automatic Synoptic Observation System (ASOS) weather stations and nine geographic regions of South Korea.

**Table 1.** Description of Coupled Model Intercomparison Project Phase 5 (CMIP5) GCMs used in this study.

No.	General Circulation Models	Atmospheric Grid [Latitude × Longitude]
1	BCC-CSM1.1	2.7906 × 2.8125
2	BCC-CSM1.1(m)	2.7906 × 2.8125
3	CanESM2	2.7906 × 2.8125
4	CCSM4	0.9424 × 1.25
5	CESM1(BGC)	0.9424 × 1.25
6	CESM1(CAM5)	0.9424 × 1.25
7	CMCC-CM	0.7484 × 0.75
8	CMCC-CMS	3.7111 × 3.75
9	CNRM-CM5	1.4008 × 1.40625
10	CSIRO-Mk3.6.0	1.8653 × 1.875
11	FGOALS-g2	2.7906 × 2.8125
12	FGOALS-s2	1.6590 × 2.8125
13	GFDL-ESM2G	2.0225 × 2
14	GFDL-ESM2M	2.0225 × 2.5
15	HadGEM2-AO	1.25 × 1.875
16	HadGEM2-CC	1.25 × 1.875
17	HadGEM2-ES	1.25 × 1.875
18	INM-CM4	1.5 × 2
19	IPSL-CM5A-LR	1.8947 × 3.75
20	IPSL-CM5A-MR	1.2676 × 2.5
21	IPSL-CM5B-LR	1.8947 × 3.75
22	MIROC5	1.4008 × 1.40625
23	MIROC-ESM	2.7906 × 2.8125
24	MIROC-ESM-CHEM	2.7906 × 2.8125
25	MPI-ESM-LR	1.8653 × 1.875
26	MPI-ESM-MR	1.8653 × 1.875
27	MRI-CGCM3	1.12148 × 1.125
28	NorESM1-M	1.8947 × 2.5

Date source: <http://portal.enes.org/data/enes-model-data/cmip5/resolution>.

### 2.3. Standardized Precipitation Evapotranspiration Index

The popularly used drought index, the Standardized Precipitation Index (SPI), employs a standardized progression of the probability distribution (e.g., gamma) related to cumulated monthly precipitation. Using a similar way, SPEI uses the difference between precipitation and potential evapotranspiration ( $D = P - PET$ ) instead of precipitation. PET estimates from the Thornthwaite [23] model were used in this study. The process of SPEI calculation discussed by Vicente-Serrano et al. [24] can be summarized as follows: the surplus accumulation of a climate water balance as the difference between the precipitation  $P$  and  $PET$  for the month  $i$ , which means deficit  $D_i$ , is calculated using Equation (1):

$$D_i = P_i - PET_i \quad (1)$$

Drought duration, the appropriate aggregation time step, is denoted by  $t_d$ . For the monthly deficit time series of  $D_i (i = 1, 2, \dots, i, i + 1, \dots, n)$ , the  $t_d$  months accumulated deficit ( $DS_i$ ) of the  $i^{\text{th}}$  month ( $i \geq t_d$ ) is obtained by Equation (2):

$$DS_i = \sum_{j=i-t_d+1}^{j=i} D_j \quad (2)$$

The water balance time series, accumulated deficit  $DS_i$ , is fitted into a log-logistic probability distribution by Equations (3) and (4):

$$g(x) = \frac{\beta}{\alpha} \left( \frac{x - \gamma}{\alpha} \right) \left[ 1 + \left( \frac{x - \gamma}{\alpha} \right) \right]^{-2} \quad (3)$$

$$G(x) = \left[ 1 + \left( \frac{\alpha}{x - \gamma} \right)^\beta \right]^{-1} \quad (4)$$

where  $\alpha$ ,  $\beta$ , and  $\gamma$  are scale, shape, and origin parameters, respectively. With  $G(x)$ , SPEI can be easily obtained as the standardized values of  $G(x)$ .

#### 2.4. Aggregation Index

Tallaksen et al. [25] defined the occurrence of a streamflow drought when the streamflow falls below the threshold level. The R–R–V approach in this study is based on a similar threshold concept using SPEI Figure 3 [26]. In Figure 3,  $d_i$  is the duration and  $v_i$  is the cumulative SPEI during the drought event. The reliability obtained from Equation (5) is the probability where the available water supply meets the water demand [27,28]. The resiliency obtained from Equation (6) is the probability that a system recovers from a period of failure. Vulnerability is the likely value of deficits ( $v_i$ ), if they occur [28]. Essentially, vulnerability expresses the severity of failures and therefore, it can be expressed as the average failure [29] using Equation (7). The vulnerability is defined as the average of total deficit, which is the sum of deficit divided by the number of deficit events. The dimensionless vulnerability is defined as vulnerability divided by the annual demand (where ‘–1’ is the demand) in Equation (8) [29]. The aggregated R–R–V index [19,30,31] for assessing the sustainability of a water system is used to quantify the overall conditions of drought event by a combination of reliability, resiliency, and vulnerability.

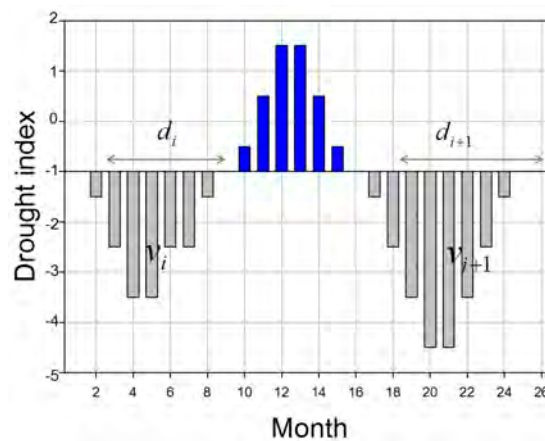


Figure 3. Severity and duration of droughts based on the threshold level.

$$\text{Reliability} = 1 - \frac{\sum_{j=1}^M d(j)}{T} \quad (5)$$

$$\text{Resiliency} = \left\{ \frac{1}{M} \sum_{j=1}^M d(j) \right\}^{-1} \quad (6)$$

$$\text{Vulnerability} = \frac{1}{M} \sum_{j=1}^M v(j) \quad (7)$$

$$\text{Dimensionless vulnerability} = \frac{1}{M} \sum_{j=1}^M v(j) / \text{annual demand} \quad (8)$$

$$\text{AI} = [\text{Reliability} \times \text{Resiliency} \times (1 - \text{Dimensionless vulnerability})]^{1/3} \quad (9)$$

where  $M$  is the total number of each drought event, and  $T$  is the number of time intervals.

### 3. Result

#### 3.1. Drought Indices for Future Drought

(1) Current: 1976–2005, (2) Future 1: 2010–2039, (3) Future 2: 2040–2069, and (4) Future 3: 2070–2099 for the analysis of the changes in R–R–V. This study defines the drought events if the values of SPEI are lower than  $-1.0$ . Based on this definition, the frequency, durations, and vulnerability of drought events were calculated and then aggregated to estimate the values of reliability, resiliency, and vulnerability. The ensemble mean of 28 GCMs' projected climate for RCP4.5 was used for the estimation of drought characteristics at each station.

##### 3.1.1. Frequency

The averaged frequencies of droughts for four periods were calculated at each station and presented in Figure 4. The drought frequencies for Future 2 and Future 3 were found similar to the frequency of the current period, while it was found higher for Future 1. The middle and northern parts showed higher frequencies for Future 1, while the southern part showed a higher frequency of droughts for Future 2 and Future 3.

The average frequencies of droughts for nine regions were calculated as shown in Figure 5. The frequency of drought in Region 5 was found to be the lowest under the current climate. Overall, droughts in the early 21st century were expected to occur more frequently than in the late 21st century. High occurrences of drought in regions 5, 6, and 7 were found for Future 1. On the other hand, the frequency of droughts in regions 3 and 9 was projected to be reduced in the future.

The box plots of drought frequencies at 60 locations for the current and future climates were prepared to investigate the changes in future drought over South Korea (Figure 6). The median frequency of droughts was found to be high in Future 1 and then decline until 2099. In Future 3, the variance of drought frequency among locations was found to increase, and the average of drought frequency was found to decrease. Overall, the results showed a decrease in the frequency of drought events, while showing an increase in the spatial variation.

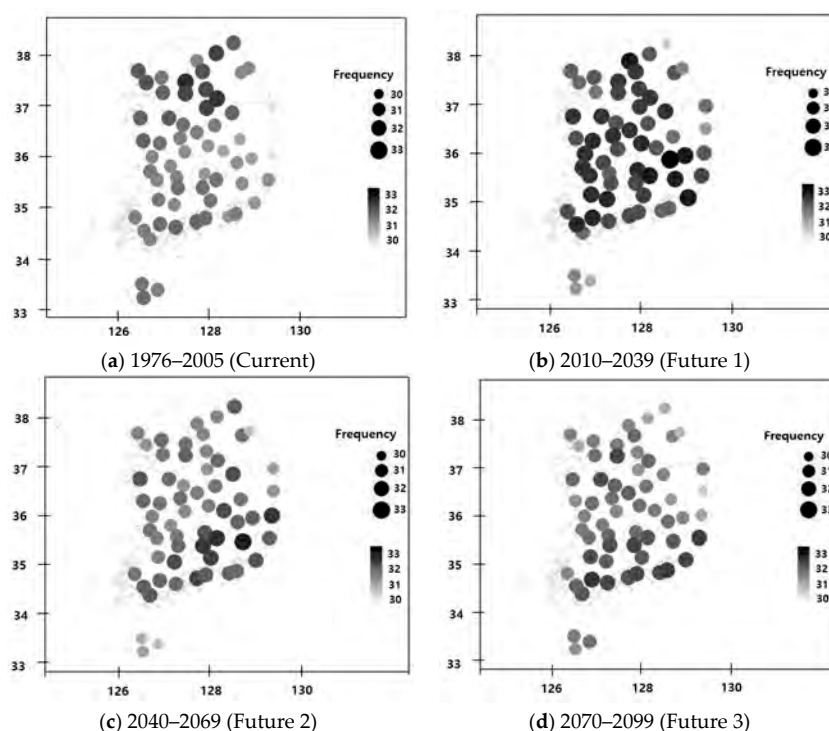


**Figure 4.** Spatial distribution of drought frequency under current and future climates.

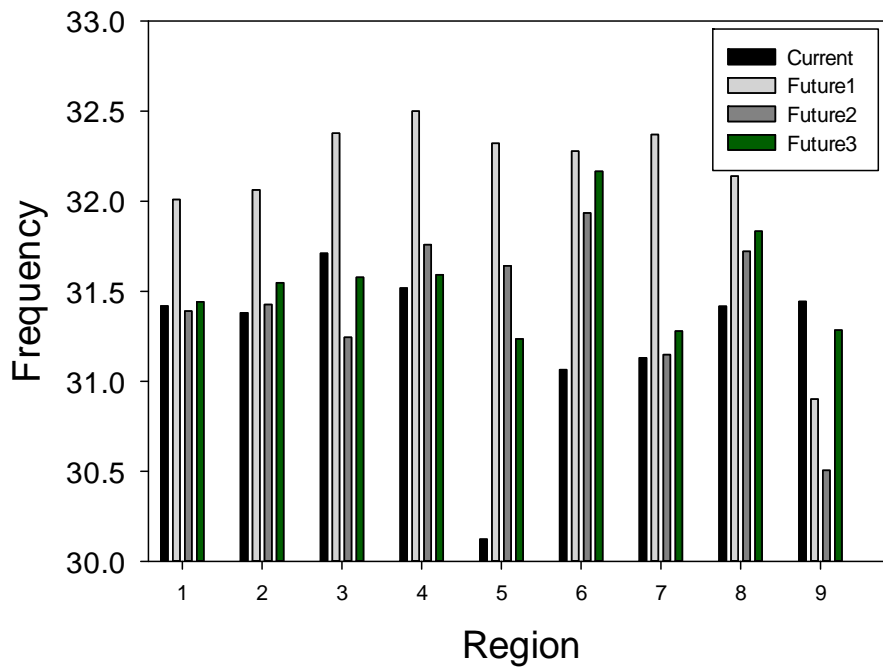


Figure 5. Average frequency of droughts in nine geographical regions of South Korea for the present and future climates.

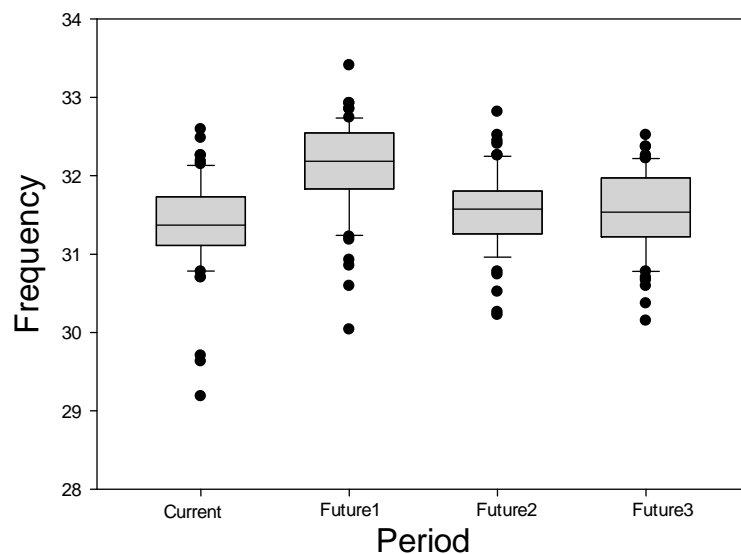
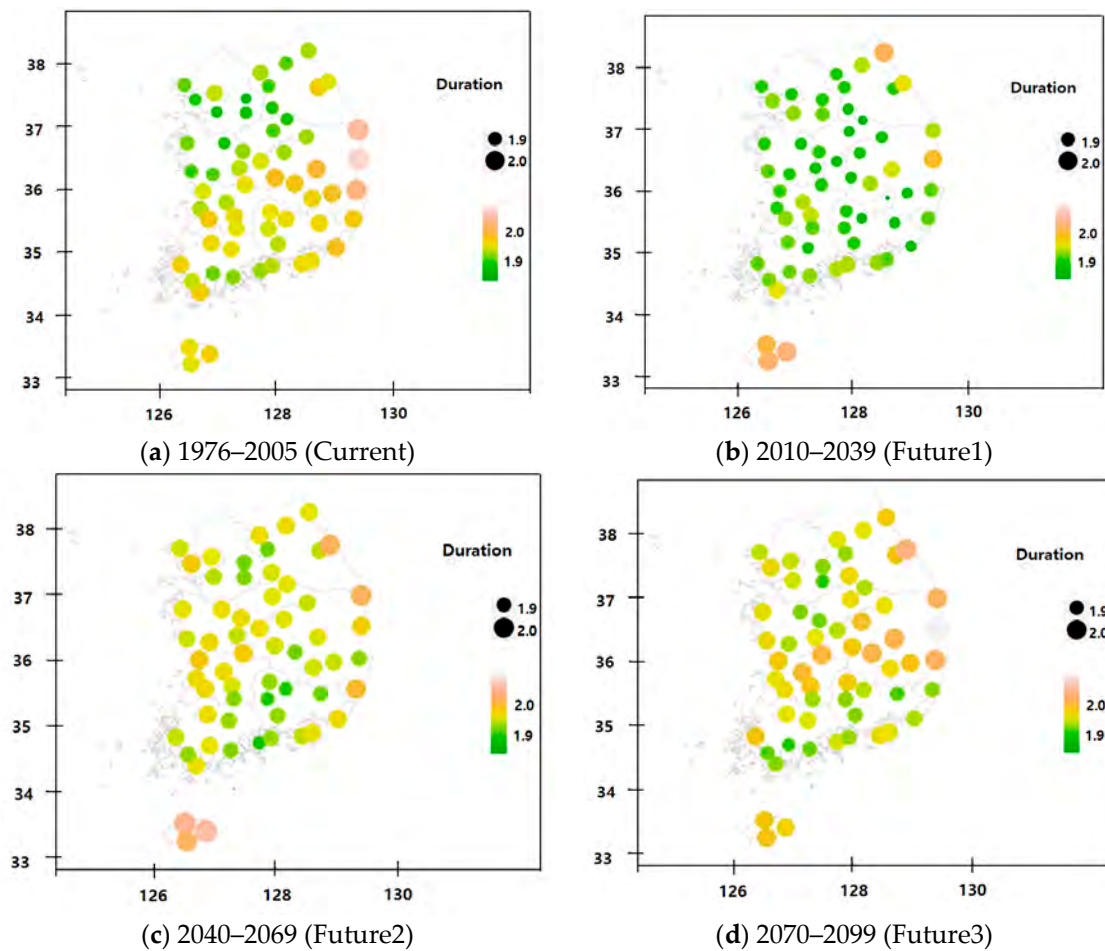


Figure 6. Boxplot of drought frequency under current and future climates.

### 3.1.2. Duration

The average drought durations for four periods at different locations are presented in Figure 7. The drought durations in Future 3 were found much larger than those in other periods. The drought durations for Future 1 were projected to be much smaller than the current climate because there are many short droughts for Future 1. This result indicated that the future drought would become longer in most of the stations as time goes by.



**Figure 7.** Spatial distribution of drought duration for present and future climate.

The average durations of droughts for eight regions are shown in Figure 8. Overall, drought durations in the future were found to be longer than in the current climate. The longer duration droughts found in Region 5 for the current climate were projected to become the longest for Future 3, while droughts in Region 6 were the shortest for all of the periods. It was also projected that the drought in Region 9 would last for a long time for Future 2. On the contrary, the drought for Future 1 would have a shorter duration than the present. In particular, it was projected that drought would frequently occur and last for a longer period in Region 5 in the future.

The box plots of drought durations at 60 locations in current and future climates are shown in Figure 9. The median duration of drought in the late 21st century was found to be long, and an increase was confirmed from the early to the late 21st century. The median and variance of duration among sites were found to increase in Future 3 compared to Future 1.



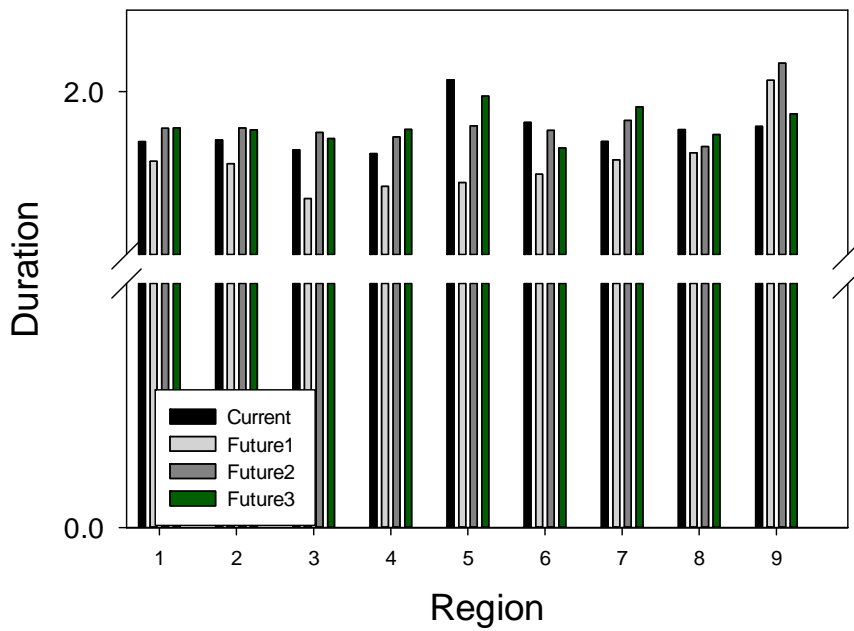


**Figure 8.** Average durations of droughts in different regions of South Korea under the current and future climate periods [month].

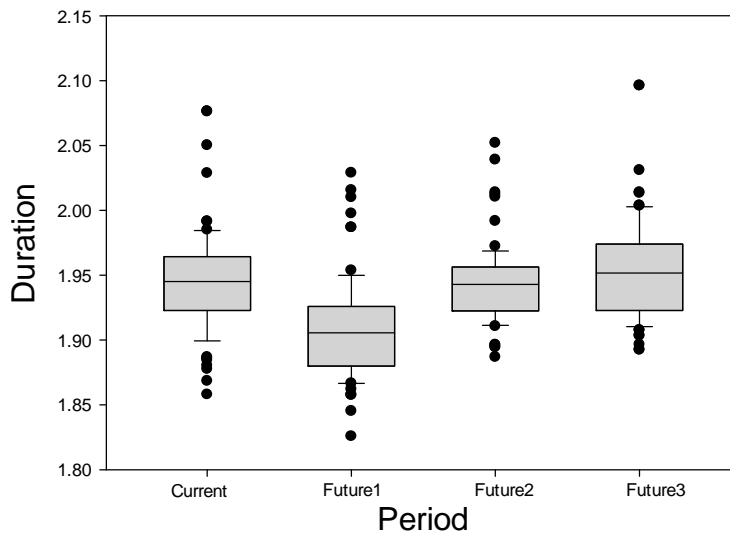


**Figure 9.** Boxplot of drought durations under current and future climate periods [month].

### 3.1.3. Severity

The average drought severities for four periods at each station were calculated as shown in Figure 10. The drought severities for Future 1 and Future 2 were found to be smaller than those for the current period. On the contrary, the drought severity for Future 3 was found to be higher than the other future periods. More severe droughts were found in the southwest region for the current climate, while more severe droughts for Future 1, Future 2, and Future 3 were projected to occur in the upper regions.

The average severity of the droughts for each region were calculated as shown in Figure 11. The results showed that the drought severity is expected to be weaker in the future compared to the current severity. However, regions 3 and 4 were projected to have more severe droughts in Future 3 than at present. The drought severities in regions 6, 7, and 8 were found to become much weaker in the future compared to the current climate period.

The box plots of drought severities at 60 locations in current and future climates are shown in Figure 12. The median severity of drought in the late 21st century during the future period was found to be high, and the variance of severity among sites were found to increase in Future 3 compared to Future 1.

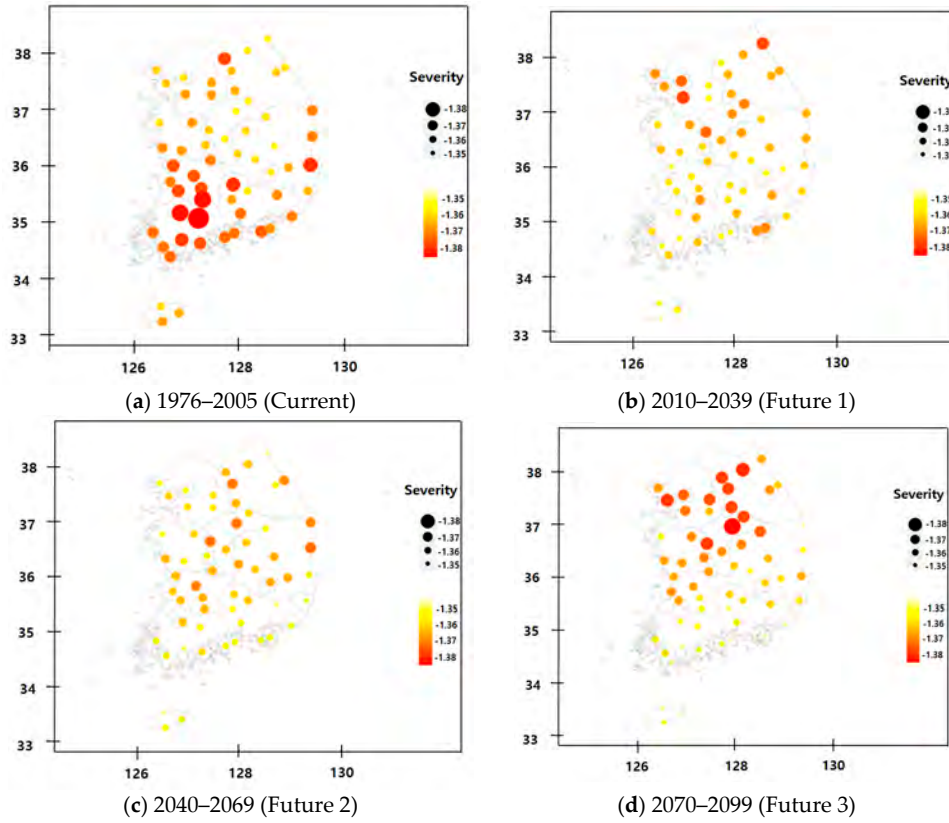


Figure 10. Spatial distribution of drought severity under current and future climates.

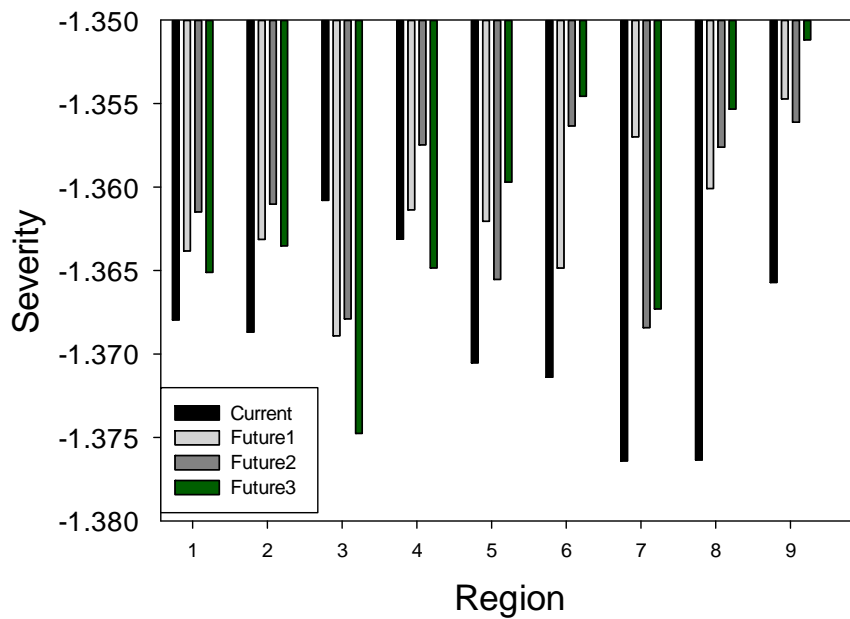
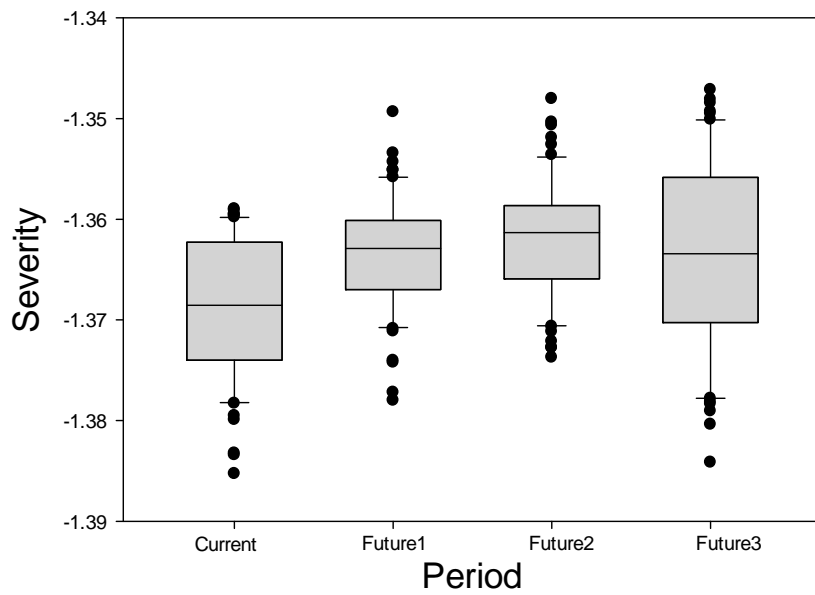


Figure 11. Average drought severities in different regions of South Korea under current and future climate periods.



**Figure 12.** Boxplots of drought severities at 60 stations in South Korea for current and future climate periods.

3.2. Projection of Aggregation Index for Future Drought

The frequency, duration, and severity of drought calculated in Section 3.1 were used to calculate the reliability, resiliency and vulnerability using Equations (5)–(7). Also, the dimensionless vulnerability was transformed from vulnerability using Equation (8). The R–R–V was calculated by aggregating the reliability, resiliency, and dimensionless vulnerability with Equation (9), and the results are shown in Figure 13. It was found that the R–R–V of Future 1 was higher than those for the current climate, Future 2, and Future 3. The R–R–V was found to gradually decrease from Future 1 to Future 3. That is, the aggregated R–R–V index will decrease, and the risk of drought will increase. For Future 3, R–R–V will be much higher than those of the current climate at half of the total stations. In addition, the spatial distribution of low R–R–Vs was projected to expand to low latitude regions in South Korea during Future 3. In particular, except for some regions of the south coast, most regions were predicted as being exposed to drought risk in Future 3.

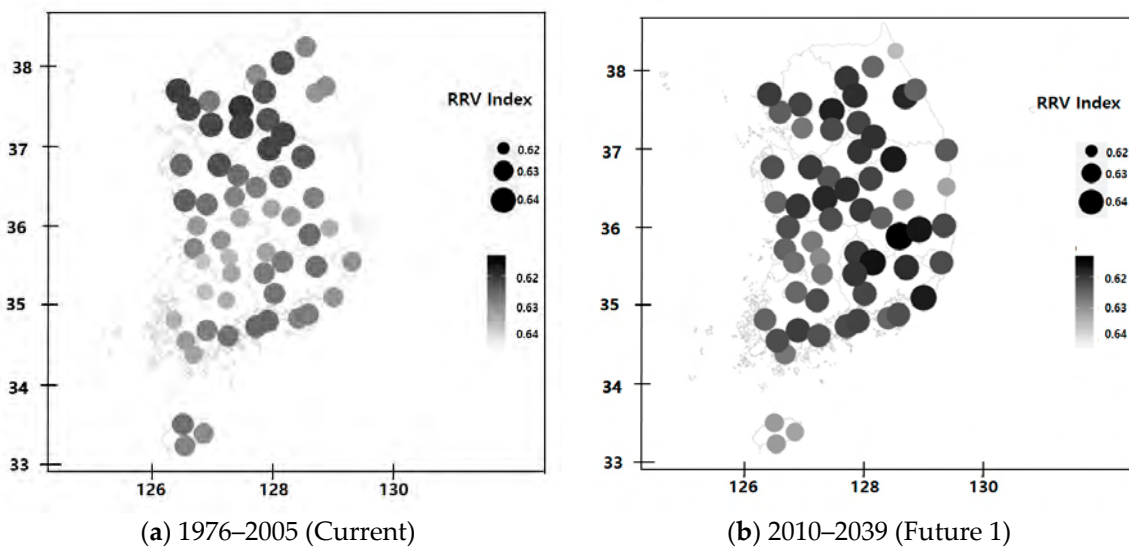


**Figure 13.** Cont.

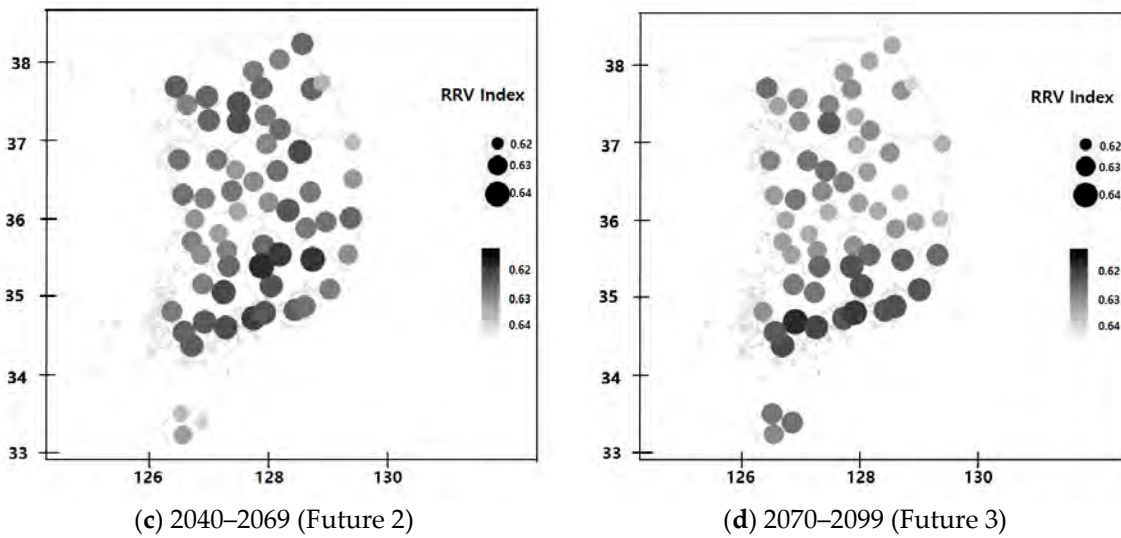


**Figure 13.** Aggregated Reliability–Resiliency–Vulnerability (R–R–V) index estimated at different stations of South Korea for current and future climate periods.

The average R–R–Vs at eight regions is shown in Figure 14. The R–R–V was projected to gradually decrease from Future 1 to Future 3 in most of the region. An increase in R–R–V was projected in Future 1 in all of the regions, and then gradually declined over time, except in Region 9. This indicates the overall decline of future drought events in South Korea.

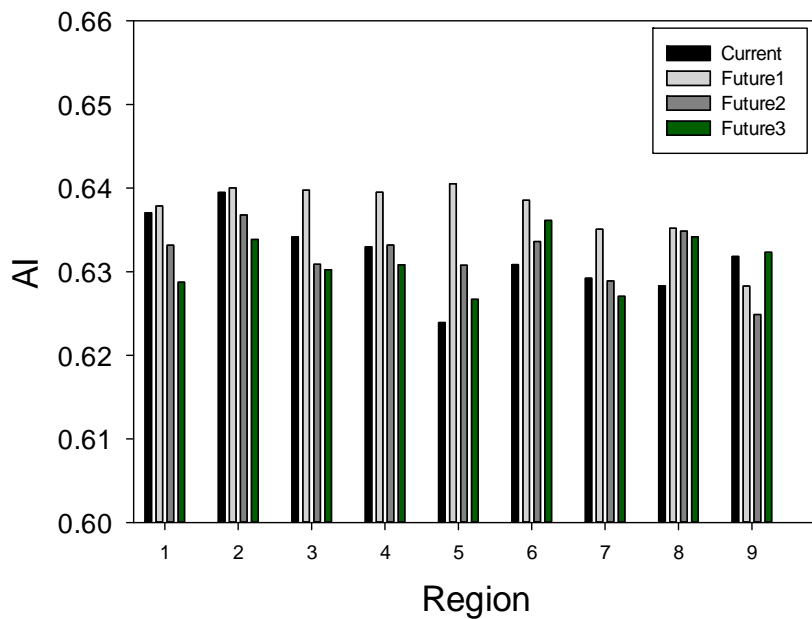


**Figure 14.** Averages of R–R–V in different regions of South Korea for the current and future climate periods.

The boxplots of R–R–V estimated at 60 stations for the current and future climate periods are shown in Figure 15. The box plots were prepared to show the changes in drought characteristics due to climate change. The ranges of the aggregated R–R–V index were 0.024, 0.022, 0.019, and 0.023 for the current climate, Future 1, Future 2, and Future 3, respectively. The median of the aggregated R–R–V index for drought in Future 1 was found the highest among all of the periods. A gradual declination of the median aggregated R–R–V index was observed for Future 1, Future 2, and Future 3, which indicates

an overall decrease in water sustainability in South Korea. The variance of the aggregated R–R–V index was also found to increase a bit for Future 1, Future 2, and Future 3. The lower whisker of the aggregated R–R–V index was prolonged for Future 1, Future 2, and Future 3, which indicates a decrease in the aggregated R–R–V index for most of the stations in South Korea.

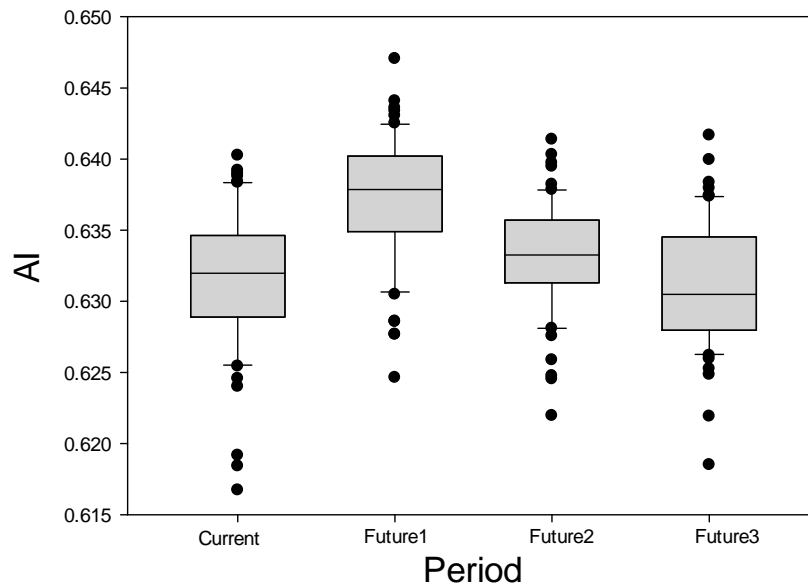


Figure 15. Boxplot of R–R–V under current and future climates.

Table 2 summarizes the changes in the frequency, duration, and severity of droughts and the aggregated R–R–V index under three future climate periods relative to the current climate. In all of the regions except Region 9, the aggregated index was found to be higher for Future 1, while in Future 2 and Future 3, they were found to be similar to that of the current climate. Although the frequency of drought was projected to increase for Future 1, the aggregated R–R–V index would increase, because the short period of drought would require a short period to recover to the normal condition. In Future 2, the aggregated index of regions 1, 3, and 9 will be lower than that of the current climate. Although the frequency of drought events was projected to decrease in these regions, the duration of drought events would be longer, and therefore more time would be required to recover to the normal state, and the drought vulnerability will increase.

Table 2. Summary of changes in the frequency, duration, and severity of droughts and the aggregated R–R–V index for three future periods relative to those for the current [%].

Region	Future 1				Future 2				Future 3			
	Fr	Dr	Sv	R–R–V	Fr	Dr	Sv	R–R–V	Fr	Dr	Sv	R–R–V
1	100.2	100.5	100.3	100.1	97.2	101.6	100.4	99.4	96.9	101.8	101.2	98.7
2	99.8	101	99.7	100.1	97.8	102.3	99.4	99.6	98.2	102	100.3	99.1
3	102.1	96.9	100.6	100.9	98.5	101.1	100.5	99.5	99.6	100.7	101	99.4
4	103.1	97.9	99.9	101	100.8	101.1	99.6	100	100.2	101.6	100.1	99.7
5	107.3	93.7	99.4	102.7	105	97.2	99.6	101.1	103.7	99	99.2	100.4
6	103.9	96.8	99.5	101.2	102.8	99.5	98.9	100.4	103.5	98.4	98.8	100.8
7	104	98.8	98.6	100.9	100.1	101.3	99.4	99.9	100.5	102.2	99.3	99.7
8	102.3	98.5	98.8	101.1	101	98.9	98.6	101	101.3	99.7	98.5	100.9
9	98.3	102.9	99.2	99.4	97	104	99.3	98.9	99.5	100.8	98.9	100.1
Average	102.4	98.3	99.6	100.9	100.6	100.3	99.5	100.3	100.6	100.6	99.6	99.9

\* Fr, Dr, and Sv means frequency, duration, and severity, respectively.

The aggregated R–R–V indices of regions 1, 2, and 3 will be lowered in Future 3, because the droughts will occur less often than those in the current climate, although the duration will be longer. On average, the frequency and duration of drought in Future 3 will be longer in South Korea, but the vulnerability will be similar to that of the current. Therefore, the risk of drought events due to drought in the future will be similar to the current.

#### 4. Conclusions

This study employed the downscaled climate projections of 28 GCMs for RCP4.5 to calculate the aggregated R–R–V index of drought. The reliability (1/frequency), resiliency (1/duration), and ‘1-vulnerability’ of droughts were projected to decrease, and the risk of drought was concluded to increase in most of the regions of South Korea. In the current period, the aggregated R–R–V index for drought was found to be relatively low, but it was projected to be lower than that for the current at about half of all of the stations used in this study for Future 3. In particular, the aggregated R–R–V indices in the northern region of South Korea (regions 1, 2, and 3) were projected to be very low in Future 3. This study also found that the frequency and duration of drought for Future 3 would be longer in the central part, such as in regions 1, 2, 3, and 4. The drought frequencies were projected to be the same in the future, but the magnitude of drought would be higher. Overall, the future drought would be prolonged, and the mean severity would be higher, despite the similar frequency.

Kim et al. [32] projected the SPEI based on the RCP8.5 scenario in the future climate, which projected that the frequency would be higher and the severity would increase in the late 21<sup>st</sup> century compared to the current climate. However, the relationship between severity and duration was not addressed in this study. We compared the duration and severity of the drought events, and then found that the magnitude increased during Future 3 compared to the current climate. The increase in magnitude results from the decrease in duration or the increase in total severity. Even though the duration in Future 3 is expected relative to the current, the large increase in total severity leads to the increases in magnitude. Nam et al. [33] projected that the duration in the late 21<sup>st</sup> century was more prolonged at RCP4.5 than at RCP8.5, and the magnitude was expected to increase toward the future based on RCP4.5 scenarios. This means that the total severity increased, which was in good agreement with our results.

It was projected that the southern part of Korea for the future would have higher aggregated R–R–V indices. The temperature in the southern region of Korea was projected to rise in the future, which will cause frequent extreme precipitations and an increase in total rainfall, and thus the risk from drought will increase. The northern region of South Korea was found to experience more extreme droughts in recent years, because the aggregated R–R–V index of the northern region is low. This region is required to cope with the drought in the long-term.

**Author Contributions:** J.H.S. conducted the study and made the first draft of the article. E.-S.C. supervised the study and helped in preparation of first draft of the article, while S.S. prepared for the final version of the article.

**Funding:** This study was supported by the Research Program funded by the SeoulTech (Seoul National University of Science and Technology).

**Conflicts of Interest:** The authors declare no conflict of interest.

#### References

1. Pew Research Center. Available online: <http://www.pewglobal.org/> (accessed on 23 July 2018).
2. Giorgi, F.; Mearns, L.O. Calculation of average, uncertainty range and reliability of regional climate changes from AOGCM simulations via the ‘Reliability Ensemble Averaging (REA)’ method. *J. Clim.* **2002**, *15*, 1141–1158. [CrossRef]
3. Doblus-Reyes, F.J.; Hagedorn, R.; Palmer, T.N. The rationale behind the success of multi-model ensembles in seasonal forecasting—II. Calibration and combination. *Tellus* **2005**, *57A*, 234–252.
4. Räisänen, J.; Palmer, T.N. A probability and decision-model analysis of a multi-model ensemble of climate change simulations. *J. Clim.* **2001**, *14*, 3212–3226. [CrossRef]

5. Rajagopalan, B.; Lall, U.; Zebiak, S.E. Categorical climate forecasts through regularization and optimal combination of multiple GCM ensembles. *Mon. Weather Rev.* **2002**, *130*, 1792–1811. [[CrossRef](#)]
6. Raftery, A.E.T.; Gneiting, F.; Balabdaoui, F.; Polakowski, M. Using Bayesian model averaging to calibrate forecast ensemble. *Mon. Weather Rev.* **2005**, *133*, 1155–1174. [[CrossRef](#)]
7. Im, E.S.; Kwon, W.T.; Ahn, J.B.; Giorgi, F. Multi-decadal scenario simulation over Korea using a one-way double-nested regional climate model system. Part 1: Recent climate simulation (1971–2000). *Clim. Dyn.* **2007**, *38*, 759–780. [[CrossRef](#)]
8. Feng, J.M.; Wang, Y.L.; Fu, C.B. Simulation of extreme climate events over China with different regional climate models. *Atmos. Ocean. Sci. Lett.* **2011**, *4*, 47–56.
9. Sung, J.H.; Kang, H.-S.; Park, S.; Cho, C.H.; Bae, D.H.; Kim, Y.-O. Projection of Extreme Precipitation at the end of 21st Century over South Korea based on Representative Concentration Pathways (RCP). *Atmosphere* **2012**, *22*, 221–231. [[CrossRef](#)]
10. Sa'adi, Z.; Shahid, S.; Ismail, T.; Al-Abadi, A.M.; Chung, E.S. Long-term trends in daily temperature extremes in Iraq. *Atmos. Res.* **2017**, *187*, 97–107.
11. Wood, A.W.; Leung, L.R.; Sridhar, V.; Lettenmaier, D.P. Hydrologic implications of dynamical and statistical approaches to downscaling climate model outputs. *Clim. Chang.* **2004**, *62*, 189–216. [[CrossRef](#)]
12. Burger, G.; Sobie, S.R.; Cannon, A.J.; Werner, A.T.; Murdock, T.Q. Downscaling Extremes: An Intercomparison of Multiple Methods for Future Climate. *J. Clim.* **2013**, *26*, 3429–3449. [[CrossRef](#)]
13. Cannon, A.J.; Sobie, S.R.; Murdock, T.Q. Bias correction of GCM precipitation by quantile mapping: How well do methods preserve changes in quantiles and extremes? *J. Clim.* **2015**, *28*, 6938–6959. [[CrossRef](#)]
14. Abatzoglou, J.T.; Brown, T.J. A comparison of statistical downscaling methods suited for wildfire applications. *Int. J. Clim.* **2012**, *32*, 772–780. [[CrossRef](#)]
15. Eum, H.-I.; Cannon, A.J. Intercomparison of projected changes in climate extremes for South Korea: Application of trend preserving statistical downscaling methods to the CMIP5 ensemble. *Int. J. Clim.* **2017**, *37*, 3381–3397. [[CrossRef](#)]
16. Xu, K.; Yang, D.W.; Xu, X.Y.; Lei, H.M. Copula based drought frequency analysis considering the spatio-temporal variability in Southwest China. *J. Hydrol.* **2015**, *527*, 630–640. [[CrossRef](#)]
17. Reddy, M.J.; Ganguli, P. Application of copulas for derivation of drought severity-duration-frequency curves. *Hydrol. Process.* **2011**, *26*, 1672–1685. [[CrossRef](#)]
18. Zongxue, X.; Jinno, K.; Kawanura, A.; Takesaki, S.; Ito, K. Performance risk analysis for Fukuoka watersupply system. *Water Resour. Manag.* **1998**, *12*, 13–30. [[CrossRef](#)]
19. Loucks, D.P. Quantifying trends in system sustainability. *Hydrol. Sci.* **1997**, *42*, 513–530. [[CrossRef](#)]
20. Thomson, A.M.; Calvin, K.V.; Smith, S.J.; Kyle, G.P.; Volke, A.; Patel, P.; Delgado-Arias, S.; Bond-Lamberty, B.; Wise, M.A.; Clarke, L.E. RCP4.5: A pathway for stabilization of radiative forcing by 2100. *Clim. Chang.* **2011**, *109*, 77. [[CrossRef](#)]
21. Kim, J.; Kim, S.; Joo, J. Analysis of drought characteristics depending on RCP scenarios at Korea. *J. Korea Water Resour. Assoc.* **2016**, *49*, 293–303. [[CrossRef](#)]
22. Gwak, Y.; Cho, J.; Jung, I.; Kim, D.; Jang, S. Downscaled climate change scenarios data for Korean Peninsula Projection of Future Changes in Drought Characteristics in Korea Peninsula Using Effective Drought Index. *J. Clim. Chang. Res.* **2018**, *9*, 31–45. [[CrossRef](#)]
23. Thornthwaite, C.W.; Mather, J.R. The water balance. *Publ. Climatol.* **1955**, *8*, 1–104.
24. Vicente-Serrano, S.M.; Begueria, S.; Lopez-Moreno, J.I. A multiscalar droughtindex sensitive to global warming: The Standardized Precipitation Evapotranspiration Index. *J. Clim.* **2010**, *23*, 1696–1718. [[CrossRef](#)]
25. Tallaksen, L.M.; Madsen, H.; Clausen, B. On the definition and modelling of streamflow drought duration and deficit volume. *Hydrol. Sci. J.* **1997**, *42*, 15–33. [[CrossRef](#)]
26. Sung, J.H.; Chung, E.-S. Development of streamflow drought severity-duration-frequency curves using the threshold level method. *Hydrol. Earth Syst. Sci.* **2014**, *18*, 3341–3351. [[CrossRef](#)]
27. Kim, Y.; Chung, E.; Jun, S.; Kim, S.U. Prioritizing the best sites for treated wastewater instream use in an urban watershed using fuzzy TOPSIS. *Resour. Conserv. Recycl.* **2014**, *73*, 23–32. [[CrossRef](#)]
28. Klemes, V.; Srikanthan, R.; McMahon, T.A. Long-memory flow models in reservoir analysis: What is their practical value? *Water Resour. Res.* **1981**, *17*, 737–751. [[CrossRef](#)]
29. Hashimoto, T.; Stedinger, J.R.; Loucks, D.P. Reliability, resiliency and vulnerability criteria for water resource system performance evaluation. *Water Resour. Res.* **1982**, *18*, 14–20. [[CrossRef](#)]

30. Loucks, D.P.; van Beek, E. *Water Resources Systems Planning and Management*; United Nations Educational, Scientific and Cultural Organization (UNESCO): Paris, France, 2005.
31. Sandoval-Solis, S.; McKinney, D.C.; Loucks, D.P. Sustainability index for water resources planning and management. *J. Water Resour. Plan. Manag.* **2011**, *137*, 381–390. [[CrossRef](#)]
32. Kim, B.S.; Sung, J.H.; Lee, B.H.; Kim, D.J. Evaluation on the impact of extreme droughts in South Korea using the SPEI and RCP8.5 climate change scenario. *J. Korean Soc. Hazard Mitig.* **2013**, *13*, 97–109. [[CrossRef](#)]
33. Nam, W.H.; Hayes, M.J.; Svoboda, M.D.; Tadesse, T.; Wilhite, D.A. Drought hazard assessment in the context of climate change for South Korea. *Agric. Water Manag.* **2015**, *160*, 106–117. [[CrossRef](#)]



© 2018 by the authors. Licensee MDPI, Basel, Switzerland. This article is an open access article distributed under the terms and conditions of the Creative Commons Attribution (CC BY) license (<http://creativecommons.org/licenses/by/4.0/>).